

Investigations on Emission Characteristics of Methane in Small Scale a Swirl Flameless Combustor: Using Preheating Air Diluted CO₂ and N₂ Gas at Various Temperatures

Abdelgader Agilah Saleh Gheidan^{1,*}, Mazlan Abdul Wahid¹, Mohd Fairus Mohd Yasin¹

¹ High-Speed Reacting Flow Laboratory, School of Mechanical Engineering, Universiti Teknologi Malaysia, 81310 UTM Skudai, Johor, Malaysia

ARTICLE INFO

Article history:

Received 10 April 2022

Received in revised form 21 September 2022

Accepted 28 September 2022

Available online 22 October 2022

Keywords:

Exhaust gas recirculation (EGR); air and fuel preheating; multi-stage air; NOx formation; computational fluid dynamics; combustion efficiency

ABSTRACT

In order to reduce the damage to the environmental, it is desirable to have low emission combustion and high-efficiency system of operation. In achieving this, the multi-stages and exhaust gas recirculation (EGR) were adopted to reduce NOx formation during combustion. In this paper, a numerical study of the impact of diluted preheated oxidizer variables on NOx emissions from methane combustion was performed. This study utilizes Computational Fluid Dynamics (CFD) analysis to determine the influence of preheating fuel and air on the combustion efficiency when asymmetric vortex flameless was applied on different supply tangential air location at different oxygen concentrations. The design parameters utilized are diluted N₂ and CO₂, oxygen concentrations of 10%, 7% and 5%, and air temperatures that were set at 300 K, 500 K, 700 K and 900 K, respectively. The exhaust gas recirculation (EGR) was simulated using CO₂ gas and N₂ gas. The results show that by oxygen concentration has direct relationship with NOx emission for all equivalence ratios. Apart from that, CO₂ dilution air offers better results than N₂ dilution in reducing NOx emissions. In terms of preheating air, higher NOx emission was observed with the increase of air temperature. However, the effect of preheating air on the NOx emission is greater than the effect of preheating of fuel. Based on these results, numerous ports were considered important to achieve a good mix of air and fuel. The analysis outcome shows that more inlet tangential air has a significant influence on combustion temperature and NOx emission.

1. Introduction

Environmental protection during combustion requires low emission combustion and high-efficiency system operations. In achieving this, multi-stages and exhaust gas recirculation (EGR) are adopted to reduce NOx formation during combustion [1–3]. The approach of (EGR) technique in controlling NOx emission has attracted the industry due to its outstanding potential in emission mitigation [4,5]. The EGR dilutes the oxygen concentration in the air stream with recirculation rates and increases the residence time, a fundamental factor for achieving flameless combustion through

* Corresponding author.

E-mail address: gheidan015@gmail.com

<https://doi.org/10.37934/arfmts.100.2.113137>

preheating the airflow [1,6,7]. Preheating of air is a technology that plays an important role in achieving flameless combustion by preheating the inlet air of the combustor before mixing it with the fuel. It also raises the temperature inside the combustion chamber above the auto-ignition temperature of the fuel to achieve flameless combustion and uniform temperature [8,9]. This combustion mode occurred by using EGR contributes in generating the desired chemical composition of the combustion air. However, the diluent gas method is another approach and plays an important role in preheating air, which can reduce NO_x emissions using exhaust gas recirculation EGR [1,7,10–12]. One way of achieving reduction in NO_x by introducing EGR in which it recirculates part of exhaust gas to the combustion chamber [1,13]. has discovered that the heat recovery system can save 21.3 % more energy than a conventional spray drying method [14].

The preheating feature helps to heat the inlet air and also to decrease the density of oxygen, which is an important key parameter to increase flow recirculation [5,9]. Also, High-temperature air combustion (HiTAC) as another approach of controlling NO_x emission is successfully used in many applications such as furnaces, gas turbines, and hybrid solar systems [15,16]. This is one of the important and effective parameters of the robust design method, which successfully reduces NO_x emissions and achieves flameless. According to Gupta [5], Mehregan and Moghiman [9], and Hosseini *et al.*, [15], energy savings of about 60% alongside pollution reductions of about 25% have been achieved. The excess enthalpy is used to establish flameless mode in the micro combustor and reduces NO_x emission. The concept of excess enthalpy is to recycle burned gas energy into the unburned gas mixture. This reduces the concentration of oxygen, increases the stability of flameless, lower particulates, uniform temperature, and reduces the formation of NO_x [5,17,18]. The mechanism works with the help of heat exchangers that recover heat from the exhaust gas. This improves thermal efficiency as well as preserving the heating and combustion reactions of a gas mixture. This technology is used to recover energy from the exhaust while simultaneously reduces emissions dramatically, leading to flameless combustion [19–21].

Another method is bluff body combustion configuration geometry, which is considered as an important technique in establishing heat recycling and reducing NO_x emissions. In the analysis conducted by Fan *et al.*, [18] and Hosseini and Wahid [22], uniform temperatures were achieved with less heat loss, quenching, and blow-out limit, leading to stable flameless and reduction in the NO_x emission generation. During the combustion assessment by Hosseini and Wahid [23], approximately 30% of the waste energy of the boiler was recovered through heat recovery from the flue gas. It is a fact that vortex interaction significantly helps in practical combustion applications by improving mixing, constructing flame zones, and improving engine performance and combustion efficiency [24–26].

There are a few techniques that can be utilized to enhance combustion and constancy, for instance vortex and swirl flame [27]. The first study on vortex flames was made by Gabler [28] in 1998 as shown in Figure 1. Generally, the strength of a vortex is defined by the number of vortices [29,30]. The NO_x emission plane in vortex combustion is lower as compared to conventional combustion [31,32]. Therefore, this study is centered on the investigations of emission characteristics of methane fuel under swirl flameless combustor by employing CO₂ and N₂ Gas as the diluent at different temperatures. The work is performed by analyzing the preheating air and fuel effect on the NO_x emission.

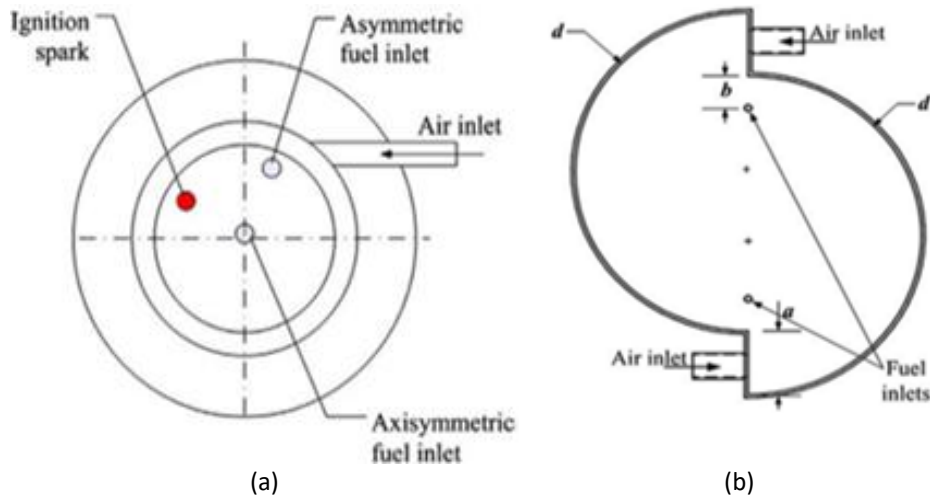


Fig. 1. Schematic of the asymmetric vortex combustor reported by (a) Gabler [28], (b) Saqr *et al.*, [33]

2. Methodology

2.1 CFD Modelling

The CFD developed for this numeral analysis relates to the combustion geometry of a previous study and uses an asymmetric combustor with tangential air inlets and axial air and fuel inlets as shown in Figure 2 [28,33]. The asymmetric vortex combustor has a dimension layout; a , b , R , and L of 4, 4, 15, and 45 mm respectively. The fuel and air inlets nozzles have a 1.5 mm diameter with a circular cross-section. Exhaust gases exit the burner through a $a = 3$ mm diameter central outlet. Figure 2 shows the asymmetric chamber design of the non-premixed forward air configuration. The design features six tangential air inlets, two axial fuels inlets, and consists of two forward axial airflows. ANSYS 16 Modeller was utilized to fabricate the flameless burner, and ANSYS Meshing was utilized in netting the burner [34]. Mesh refinement, together with scalar characteristics, can be enhanced, and grid resolution can be ensured for stable flow. The number of mesh grids has a direct effect on the time it takes to solve a problem. The control volume meshes close to the air and fuel nozzles are tiny to improve the accuracy of predictions as shown in Figure 3. Figure 4 shows the plots of central axis temperature along with the axial position for four various meshes. M1 consists of 153,212 cells, while M2 consists of 197,181 cells. Tetrahedral elements were used to make M3=305,729cells and M4=626,282 cells. Simulation data was obtained for different meshes when the preheated air temperature was set to 900 K and the oxygen level of the oxidizer was set to 7%. The simulation results with M3=305,729 cells are good and agree with the accuracy and saves time. The grid was tested independently in the emulation by converting the amount of nodes to smaller meshes.

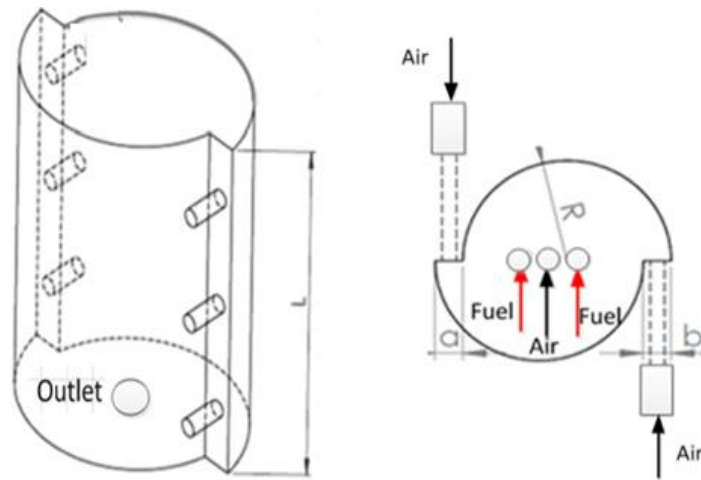


Fig. 2. The schematic of vortex flameless chamber

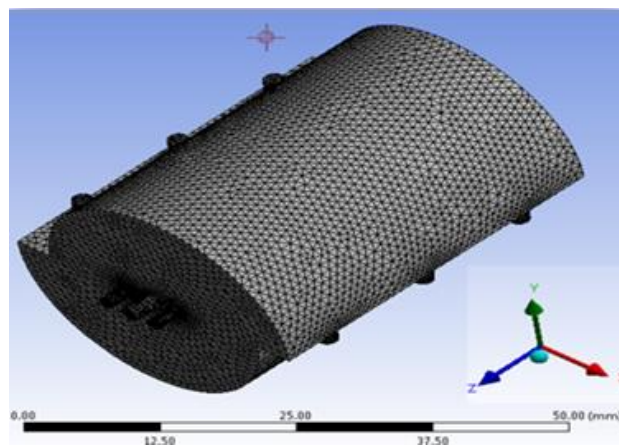


Fig. 3. Mesh mesoscale flameless combustion

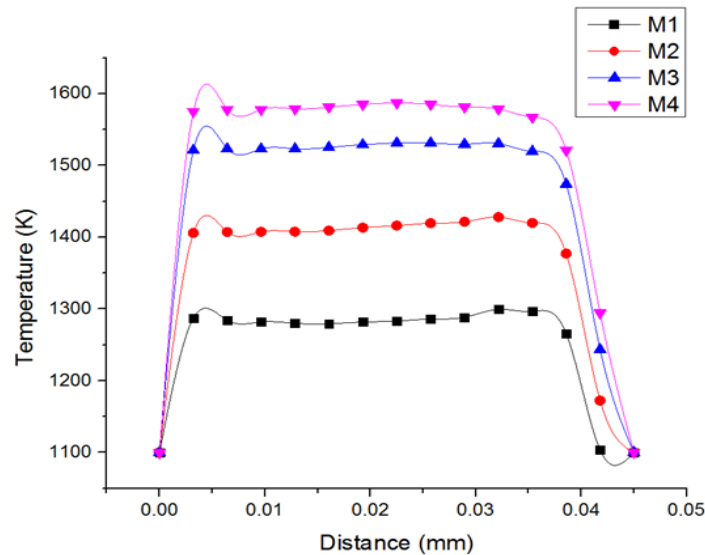


Fig. 4. Grid independence test

The CFD package ANSYS FLUENT16 [34] was used to dissolve the governing equations (transport equations such as continuity, energy, and momentum). The 3D conservation equations are given below for mass, momentum, and also energy [35-37]. The mass conservation is given as

$$u_i = \bar{u}_i + \acute{u}_i \quad (1)$$

$$\frac{\partial \rho}{\partial t} + \frac{\partial}{\partial x_i} (\rho u_i) = 0 \quad (2)$$

ρ and u_i are density and flow velocity in the i-direction respectively. The momentum equation is stated as

$$\frac{\partial \rho}{\partial t} \rho u_i + \frac{\partial}{\partial x_i} \rho u_i u_j = \frac{\partial p}{\partial x_j} + \frac{\tau_{ij}}{\partial x_i} + \rho \sum_{K=1}^N Y_K f_{K,j} \quad (3)$$

The viscous tensor $\tau_{i,j}$ is expressed as

$$\tau_{ij} = -\frac{2}{3} \mu \frac{\partial u_k}{\partial x_k} \delta_{ij} + \mu \left(\frac{\partial u_i}{\partial x_j} + \frac{\partial u_j}{\partial x_i} \right) \quad (4)$$

Where ρ , Y_k , $f_{k,j}$ stands for the pressure, the species k mass fraction, along with the volume force that acts on the j direction of the species (k) respectively, while δ_{ij} and μ indicate the Kronecker symbol and the dynamic viscosity respectively. The energy equation is given as:

$$\rho C_p \frac{dT}{dt} = \dot{\omega}_T + \frac{\partial}{\partial x_i} \left(\lambda \frac{\partial T}{\partial x_i} \right) - \left(\rho \sum_{K=1}^N C_{p,k} Y_k V_k \right) \frac{\partial T}{\partial x_i} + \tau_{ij} \frac{\partial u_i}{\partial x_j} + Q + \rho \sum_{K=1}^N Y_K f_{K,j} V_{kj} \quad (5)$$

where variables C_p , T , and λ represent the mass heat capacity, the temperature, the thermal conductivity of the mixture. While $\dot{\omega}_T$, $C_{p,k}$, and Q are the rate of heat release, the mass heat capacity of species k , and the heat source term.

$$\frac{\partial \rho Y_k}{\partial t} + \frac{\partial}{\partial x} (\rho (u_i + V_{k,i}) Y_k) = \dot{\omega}_K \quad (6)$$

where $V_{k,i}$ and $\dot{\omega}_K$ stand for the species k in the direction i and the reaction rate of species k diffusion each velocity. By assuming every species is fixed in the gas state, it can be conjectured that the optimum gas behavior is for all species. In this stable condition of the CFD model, biogas was used as the fuel while the equivalent ratio was a variable for non-premixed flameless combustion mode. The equivalence ratio was used to determine whether a chemical reaction's fuel-air mixture is lean (Φ), stoichiometric ($\Phi = 1$), or rich ($\Phi > 1$) [38]. In 300 K, the density of CH_4 is 0.6682 kg/m^3 . Table 1 shows the densities of preheated air at varying temperatures and with different N_2 and O_2 mixtures. By altering the air and fuel inlet mass flow, the equivalences ratio was regulated as shown in Table 2. Methane-air-2step was used to model the species transport and calculated by the following equations [39].



In the chemical reaction of Eq. (8) carbon monoxide (CO) and water vapor (H_2O) are produced, whereas in Eq. (9), CO is oxidized to CO_2 and the separation occurs. A chemical process for Combustion Chemistry Modelling consists of at least three segments: a gas-phase kinetic order (a

collection of every wanted chemical reaction in simulation, among other things relevant Arrhenius coefficients), a thermodynamic database (thermodynamic coefficients of every gas-phase kinetic file), and a transport data order. The coefficients utilized in Eq. (7) and Eq. (8) are the coefficients of the Arrhenius equation.

$$k = AT^\beta e^{-\left(\frac{E}{RT}\right)} \quad (9)$$

where k denotes reaction rate, R denotes gas constant, A denotes pre-exponential, T denotes temperature, and β denotes a dimensionless number of orders one. The heat loss from the wall to the surroundings was also calculated by Eq. (10), Both thermal radiation and normal convective heat transfer were investigated [40].

$$q = h(T_{s,o} - T_\infty) + \varepsilon S(T_{s,o}^4 - T_\infty^4) \quad (10)$$

where $T_{s,o}$ denotes the outer surface temperature, T_∞ denotes the ambient temperature set at 300 K, h denotes the natural convection coefficient with a deliberated constant value 5 W/m² K, $\sigma = 5.67 \times 10^{-8}$ W/m² K⁴ denotes Stephane- Boltzmann constant and e denotes the solid surface emissivity.

According to previous studies on macro-scale flameless combustion technology, the dilution of oxidants is often referred to as one of the flameless formation fundamentals [41,42]. These studies established that if the oxygen concentration in the combustion air rises to 15%, a flame is formed. The parameter for this experiment was chosen with regards to the previous macro-scale flameless mode experiments. The oxidizer temperature in conventional combustion (21% O₂ and 79% N₂ by vol.) is 300 K, while the inlet oxidizer temperature in flameless combustion (case1: 5% O₂ and 95% N₂, case2: 7% O₂ and 93% N₂, and case3: 10% O₂ 90% N₂ by vol.) is 900 K, which is greater than methane's self-combusting temperature.

Table 1
 Air density (kg/m³) in different temperatures

Temperature (K)	5% O ₂	7% O ₂	9% O ₂	10% O ₂	21% O ₂
300	1.146	1.15	1.152	1.154	1.177
500	0.687	0.689	0.691	0.692	0.7063
700	0.491	0.492	0.4937	0.4946	0.5046
900	0.382	0.383	0.3841	0.3847	0.3925

Table 2
 Medium parameters used in the investigatory analysis

No.	Φ	m_a kg/s	m_F kg/s
1	0.5	2.7652×10^{-6}	2.828×10^{-7}
2	1	2.7652×10^{-6}	5.655×10^{-7}
3	1.2	2.7652×10^{-6}	6.785×10^{-7}

2.2 Numerical Analysis Conditions

In the present analysis, a finite volume of the three-dimensional solver was used in FLUENT 16.0 to study the continuous and non-premixed combustions. The spatial discretization of mass, momentum, and energy transport equations were presented in the second-order upwind scheme. The methane-2 step reaction mechanism designs were adopted based on the volumetric chemical reactions. Turbulent-chemical interactions were also modeled with eddy dissipation models [34]. The

boundary conditions of this analysis had been selected based on the previous experiments in macro-scale flameless mode [23]. The temperature of 900 K for the inlet oxidizer (case1: 5% O₂ and 95% N₂, case2: 7% O₂ and 93% N₂, case3: 10% O₂ and 90% N₂ by vol.) was adopted in the meso-flameless mode, which was higher than the methane self-ignition temperature. The inlet temperature of CH₄ and the oxidizer was 300 K. The effects of the preheated oxidizer and fuel ($T_{inlet} = 300, 500, 700, 900$ K), as well as the equivalence ratio ($\Phi=1$), were simulated to study the different aspects of combustion on NO_x emission. Besides, the effect of diluted oxidizer factors (N₂ and CO₂) on NO_x emissions at variable temperatures of inlet air ($T_{inlet\ air} = 300, 500, 700, 900$ K) and constant oxygen concentration at (7% O₂) were analyzed. Table 3 and Table 4, respectively, show the description of the boundary conditions for the inlet oxidant and the boundary conditions for the fuel inlet, wall, and pressure outlet. The general simulation is shown in Table 5. For estimating the O₂ radical concentrations needed for thermal NO_x prediction, partial equilibrium models were applied. In consecutive iterations, if the residual in each equation is less than 1×10^{-6} , the solution is considered to converge, which was carried out by applying grid independence tests. M3=305,729 cells with a minimum cell size of 0.003 mm per grid independence test are shown in Figure 3.

Table 3

The boundary conditions of inlet oxidant

Oxidizer inlet	
Temperature	($T_{inlet\ air} = 300, 500, 700, 900$ K)
Gauge Pressure	0
Hydraulic diameter	1.5 mm
Turbulent intensity	10
Oxygen concentration	5%, 7%, 10%
Density (ρ) Kg/m ³	Variable with temperature air inlet and oxygen concentration
5% O ₂ concentration	$\rho = (1.146, 0.687, 0.491, 0.382)$ kg/m ³
7% O ₂ concentration	$\rho = (1.15, 0.689, 0.492, 0.383)$ kg/m ³
10% O ₂ concentration	$\rho = (1.154, 0.692, 0.4946, 0.3847)$ kg/m ³

Table 4

The boundary conditions of fuel inlet, wall, and pressure outlet

Fuel inlet	Temperature	($T_{inlet\ fuel} = 300, 500, 700, 900$ K)
	Hydraulic diameter	1.5 mm
	Turbulent intensity	10
	Fuel	CH ₄
	Density	0.6682 kg/m ³
	Mass flow rate	Variable
Wall	Wall slip	Non-slip
	Material	Steel
	Heat transfer convection	5 W/m ² k
Pressure outlet	Hydraulic diameter	3 mm
	Turbulent intensity	5

Table 5
Initial Settings of simulation

Viscous model	k–e Standard
Radiation model	Discrete ordinate (DO)
Combustion model	Species transport
Mixture properties	Methane–air
Turbulence chemistry interaction	EDM Volumetric
Reaction	Thermal NOx
NOx	Prompt NOx

HITAC is applied as an (EGR) technique to the flue gas energy lost from the chamber chimney. The efficiency of combustion in the HiTAC method is therefore greatly improved [7,21,43]. In Eq. (11), the efficiency of the HiTAC technique is evaluated by the recirculation ratio (Kv).

$$Kv = \frac{M_e}{M_a + M_f} \quad (11)$$

where M_e is the exhaust gas flow rate before the reaction in the equation, M_f is the fuel flow rate, and M_a is the oxidizing flow rate [21,43]. To have a flameless mode, the temperature of the chamber must be heated above the mixture's self-ignition. Thus, in the first stage, the mechanism must function by using conventional combustion. This is accomplished by a heavy dilution of the reactants by the depleted gases (exhausted gases rich in N_2 and CO_2). In these conditions, visible and audible flames vanish, and the reaction zone extends across the combustion chamber [21,41,43].

2.3 Study of Tangential Air Location Inlet on Swirling Flameless Combustion

In this vortex-combustion study, seven injection positions for air and two fuels were investigated. The swirling airflow was created through six tangential air injections, and the combustor was operated in methane at stoichiometric equivalent ratio ($\Phi=1$) and injected perpendicular to the airflow (distributed in the circumferential direction). The obtained results were divided into three groups according to the number of air inlet ports (7 ports) and two fuel inlets.

2.4 Model Validation

Validation of the model was carried out by considering boundary and geometry conditions as done by Wu *et al.*, [44]. Air flowed to the asymmetric combustor (300 K) with full tangential velocity components and fuel was performed at an equivalent ratio of $\Phi = 1$. Six tangential air flows, two axial air, and two axial fuel inlets were used. The air inlet's mass flow rate of 2.7652×10^{-6} kg/s was taken when k-epsilon Eq. (1) RNG was selected as the turbulence model reaction cases under dissimilar turbulence models and performed for comparison effects. By comparing the results with the experimental correlations of other turbulence models, further testing of the validity of the code was performed according to Khaleghi *et al.*, [45] and Saqr *et al.*, [46]. Compared to the experimental records, the axial temperature distribution of the present investigation shows a good result of the simulated data, thus, similar to the reported findings provided by the experimental records [9,24,47–49]. Besides, the change in the distribution of axial temperature with oxygen concentrations was investigated using the experimental data according to a previous study [49]. The temperature distribution and the formation of NOx emissions when applying various oxygen concentrations (5%,7%, and 10%) were compared with the previous experimental study by Gupta *et al.*, [50] and Abuelnuor *et al.*, [51]. Compared to the experimental records, CO_2 dilution is more effective in NO

reduction as compared to N₂ at the same recirculation ratio of dilution gas [52-56]. An investigation was carried out to study the effect of preheating air more than the effect of preheating fuel on temperature and NO_x emission as according to previous results [25]. The study examined multi-injection locations for air and fuel. NO_x concentrations were greater when multi-port air inlets were used relative to other air inlets with fewer ports as according to the previous study [30,57,58].

2.5 Study on Diluents of CO₂ and N₂ On Combustion Temperature and NO_x Emission

To measure the efficiency of the meso-flameless combustion under different situations, an investigation was performed on two different cases (case one: N₂ was utilized as a diluent, case two: CO₂ was utilized as a diluent) at the same O₂ concentration (7%). The combustion temperatures considered in this research were 300 K, 500 K, 700 K, and 900 K. The mass flow rate and equivalent ratios of the air and fuel inlets remained constant at 2.7652×10^{-6} kg, 5.65985×10^{-7} kg/s, and ($\Phi=1$), respectively. The current research simulates EGR in the air by providing the combustion air with the required chemical composition. In general, the combustion dilution means that, by combining the fuel and oxidant with inactive gases such as CO₂ and N₂ before the start of the burning phase, the concentration of oxygen in contact with the reactants is slightly lower than the normal air (21%).

3. Results and Discussion

3.1 Effect of Different Oxygen Concentration (%) on Combustion Temperature and NO_x Emission

Figure 5 shows the investigation results of the temperature distribution and the formation of NO_x emissions when applying different oxygen concentrations (5%, 7%, and 10%) with diameters of 2 mm and 1.5 m for the air and fuel inlets. The mass flow rate and equivalent ratio of air and fuel inlets remain constant at 2.7652×10^{-6} kg/s and 5.65985×10^{-7} kg/s at stoichiometric equivalent ratio ($\Phi=1$). The generated data shows that by increasing the concentration of oxygen with a steady mass flow rate increases the temperature gradient. The obtained result is similar to the findings generated by [9,41,51,59]. Consequently, NO_x emissions increase as the combustion temperature increases. More so, oxygen concentration exhibits a significant role in establishing flameless combustion. The used of EGR to dilute the oxygen concentration in the air mixture was adopted. As stated earlier, diluent gas is another important way to achieve flameless combustion to reduce NO_x emissions using EGR. The current analysis simulates EGR in the air by supplying the desired chemical composition to the combustion air [60,61]. Analysis was performed for the emission levels at a temperature of 300 K and O₂ concentrations of 5%, 7%, and 10%. The results indicate high NO_x emissions with the increase of O₂ concentrations at a constant temperature of 300 K.

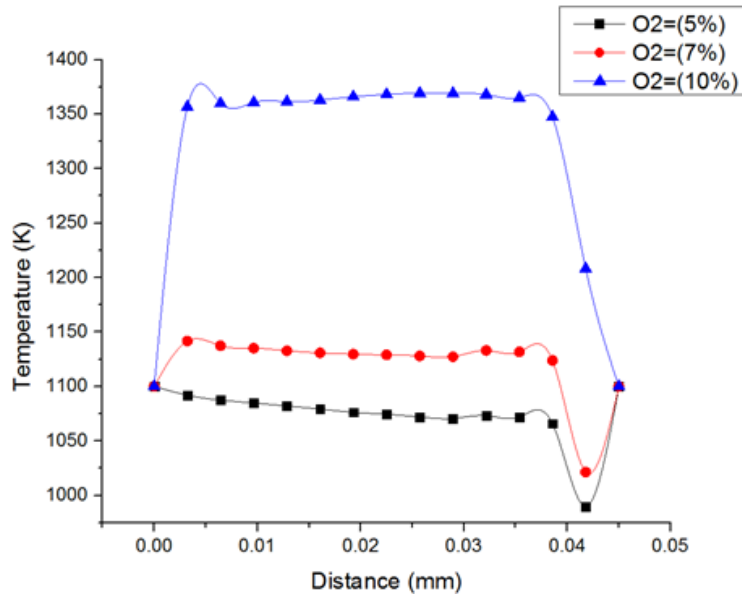


Fig. 5. Effect of oxygen concentration (%) on the profile of central temperature

The images represent the influence of oxygen concentrations on temperature combustion and NO_x emissions are presented in Figure 6, Figure 7(a), Figure 7(b) and Figure 7(c) with an oxygen concentration of 5%, 7%, and 10%, respectively. The results indicate a significant increase in NO_x as O₂ concentration increases.

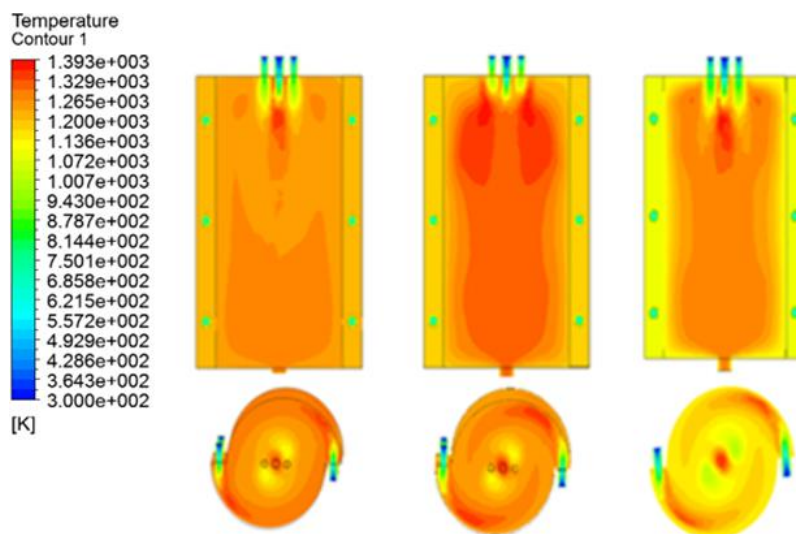


Fig. 6. Flameless combustion production at different oxygen concentrations (O₂ = 5%, 7%, and 10%)

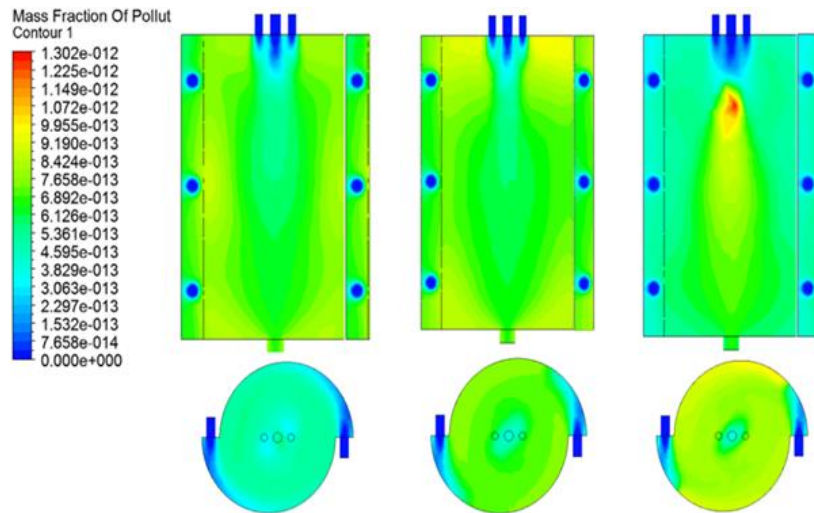


Fig. 7. Flameless combustion production at different oxygen concentrations ($O_2 = 5\%$, 7% , and 10%)

An increase in oxygen concentration has increased the combustion temperature and NO_x emissions as shown in Figure 8. The concrete finding also reveals that at equivalent ratios Φ (1 and 1.2), the oxygen concentration has a minimal effect on NO_x , while the oxygen concentration has a significant effect on NO_x at equivalent ratio ($\Phi=1$) ($O_2 = 10\%$) as shown in Figure 9.

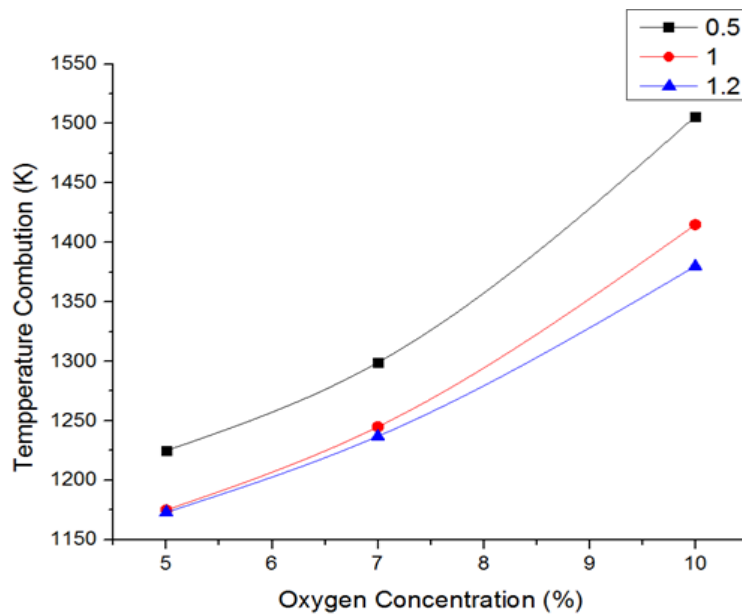


Fig. 8. Effect of oxygen concentration (%) on temperature at ($\Phi = 0.5, 1$ & 1.2)

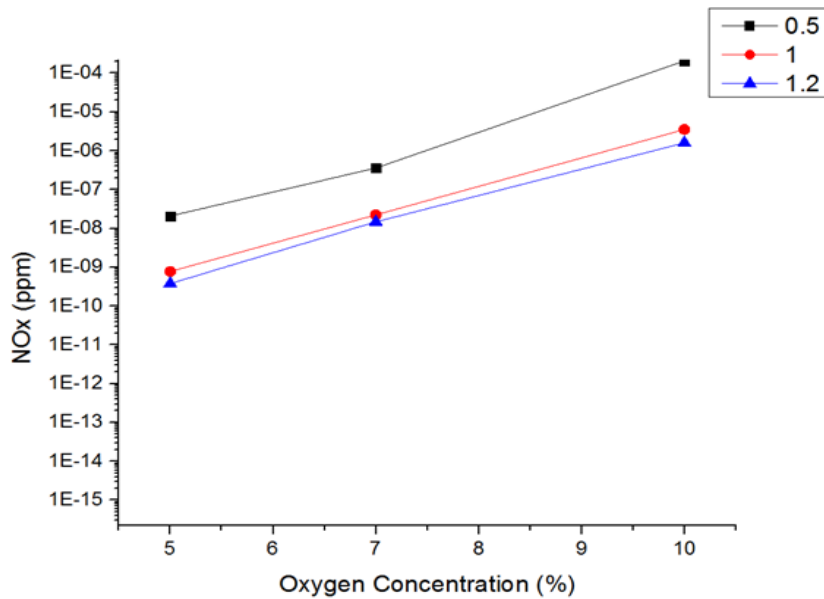


Fig. 9. Effect of oxygen concentration (%) on NOx emission at ($\Phi = 0.5, 1$ & 1.2)

3.2 Effects of Preheating Air

Flameless combustion in reconditioned furnaces by employing high preheated air has attracted a lot of attention for its ability to save energy while also emitting ultra-low NOx emissions [5,9,16,20].

Figure 10 and Figure 11 demonstrate the distribution of temperature and production of NOx contaminants when oxidizer (7% O₂ and 93% N₂) was applied at four air temperatures (T = 300, 500, 700, 900 K) with the diameter of 2 mm and 1.5 m of the air inlet and the fuel. The mass flow of the inlet mixture (air and fuel) and equivalent ratios stay constant at 2.7652×10^{-6} kg/s, 5.65985×10^{-7} kg/s, and 1, respectively. On the central axis, all predictions were carried out in the same position as stated in the conditions above. It is observed that the higher temperature of the preheated air decreases the air density and increases the uniformity of the furnace temperature. This result is similar to the observations made by Mehregan and Moghiman [9], Abuelnuor *et al.*, [51]. Furthermore, the findings show that by rising the preheating air temperature with a constant mass flow rate increases the temperature of combustion as shown in Figure 10. As a result, NOx emissions increase as the preheated air temperature increases as shown in Figure 11.

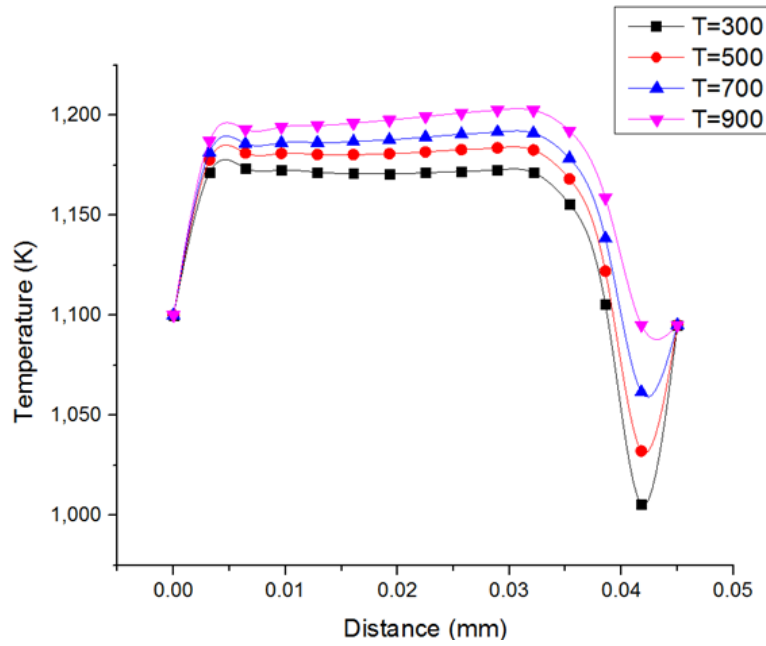


Fig. 10. Effect of preheating air on the profile of the central temperature

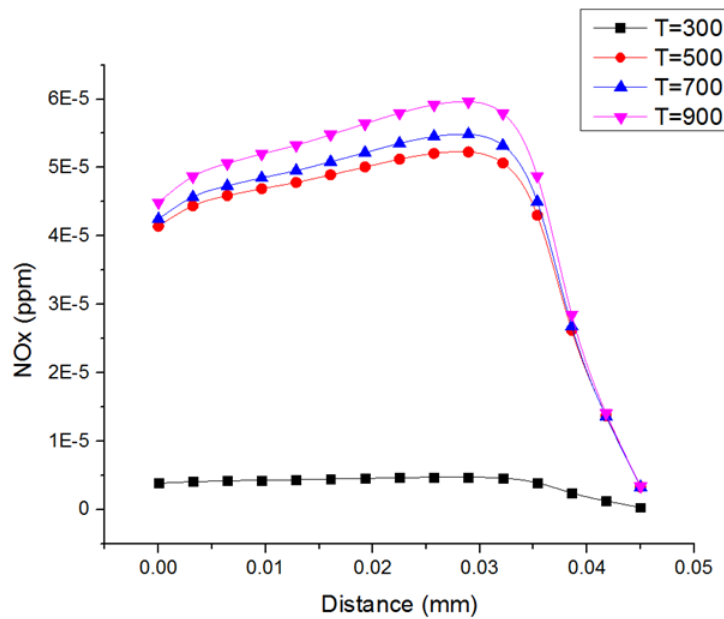


Fig. 11. Effect of preheating air on the central (a) NOx profile

By increasing the temperature of preheated air often leads to more NO_x emissions hence gives the same result as the previous presentations [9,51,62]. NO_x emissions are around 5×10^{-7} ppm at the lower temperature of 300 K at 7% of O₂ and $< 5.5 \times 10^{-5}$ ppm at the temperature of 900 K as shown in Figure 11. This observation is due to an increase in the inner temperature of the burner, which leads to more formation of NO_x as shown in Figure 12.

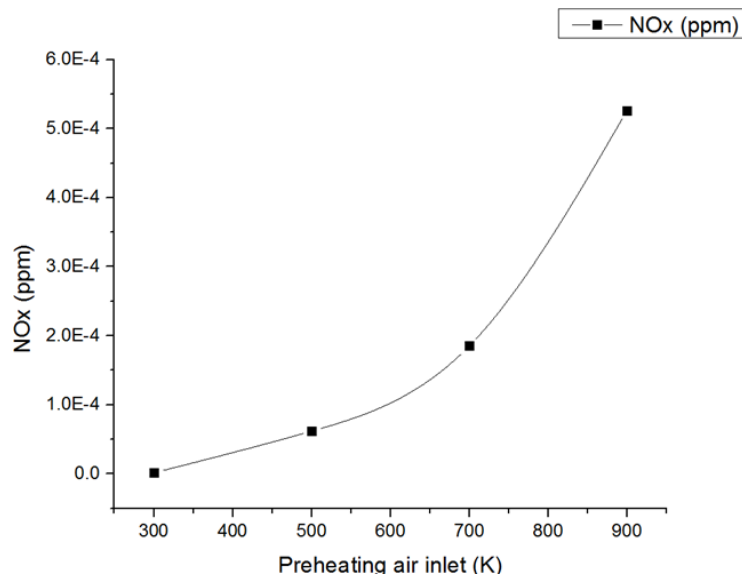


Fig. 12. Effect of preheating air on the NOx emission

3.3 Effects of Preheating Fuel

One of the strategies that contribute to establishing flameless combustion is by preheating the fuel. Preheated fuels are receiving renewed attention due to their ability to save energy along with ultra-low NOx emissions [25,63].

Figure 13 and Figure 14 depict the distribution of temperature and NOx emission generation when the fuel was used at four specific temperatures ($T= 300, 500, 700, 900$ K) with a diameter of 2 mm and 1.5 m for the air inlet and the fuel. The mass flow of the inlet mixture (air and fuel) and equivalent ratios stay constant at 2.7652×10^{-6} kg/s, 5.65985×10^{-7} kg/s and ($\Phi=1$) respectively, and oxidizer (7% O_2 and 93% N_2) was used at constant temperatures of ($T = 300$). The result shows that as the fuel temperature increases, the temperature within the centre of the axis of the combustion chamber has not significantly changed as shown in Figure 13. The distribution of temperature is uniform and decreases in all states towards the combustor outlet due to the recirculation. It increases the fuel-air mixing, which decreases the high domestic temperature zone in operation.

Figure 14 shows that as the temperature of the inlet fuel rises, the increasing temperature of flameless combustion contributes to a rise in NOx emissions through preheating the fuel at the preheating levels temperatures (300, 500, 700, and 900 K). The distribution of NOx emissions along the central axis of the combustor where the emission of NOx under the stoichiometric condition ($\Phi=1$) and temperature of 900 K is higher than NOx emissions at other temperatures, which are less than 900 K at same conditions. The preheating fuel temperature has a minimum effect on the distribution of NOx emissions along the central axis of the combustor at various temperatures as compared to NOx emission distribution through preheating air under the same condition of various temperatures, as shown in Figure 11 and Figure 14 [25].

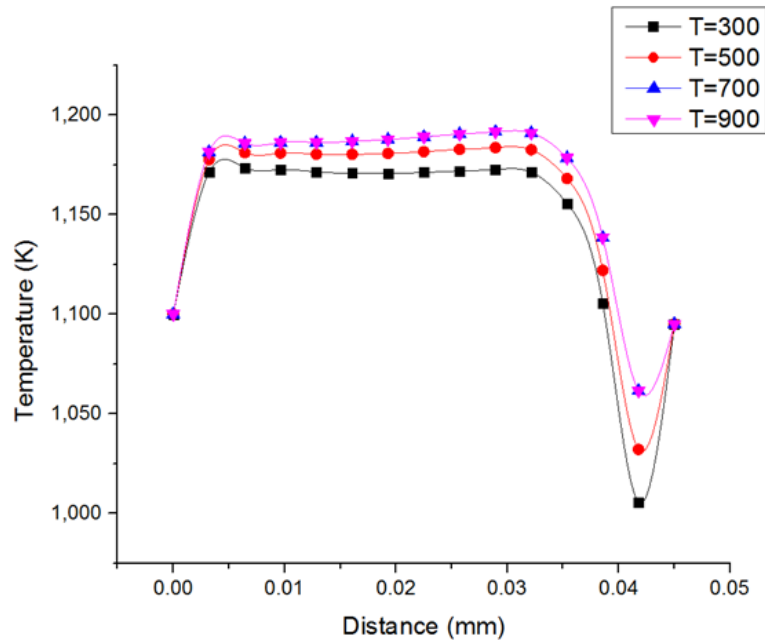


Fig. 13. Preheating fuel influence on the profile of central

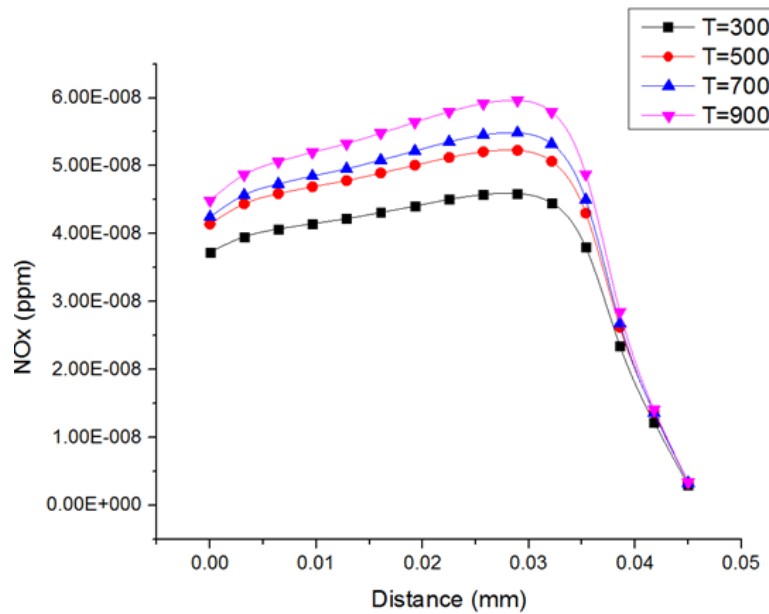


Fig. 14. Preheating Fuel influence on the central (a) NOx profile

Figure 15(a) and Figure 15(b) show the effect of preheating fuel and air on the flameless combustion features such as temperature condition and NOx emissions at various temperatures. The mass flow of the inlet mixture (air and fuel) and equivalent ratios are constant at 2.7652×10^{-6} kg/s, 5.65985×10^{-7} kg/s, and ($\Phi=1$), respectively and oxidizer (7% O₂ and 93% N₂). As the temperature of the preheated air increases, NOx emissions have been observed to increase with temperature as compared to the preheated fuel, which shows the minimal effect on temperature and NOx emissions. The maximum NOx emission of 2.2×10^{-4} ppm is achieved at a preheated air temperature of (T=900) with the maximum combustion temperature of 1456 K. In contrast, the maximum NOx emissions of preheated fuel is 8.2×10^{-7} ppm and 1358 K of combustion temperature. However, preheating has more influence on NOx emissions and increases the temperature of combustion in the case of preheating air as compared to preheating fuel as shown in Figures 15(a) and Figure 15(b). All results

are consistent with previous studies [25,63]. Preheated air is a technology that plays an important role in establishing flameless combustion and improving the efficiency of the system. The result from Figure 15(a) and Figure 15(b) show that preheating shows more effect on the air system than fuel as illustrated in the graph curves.

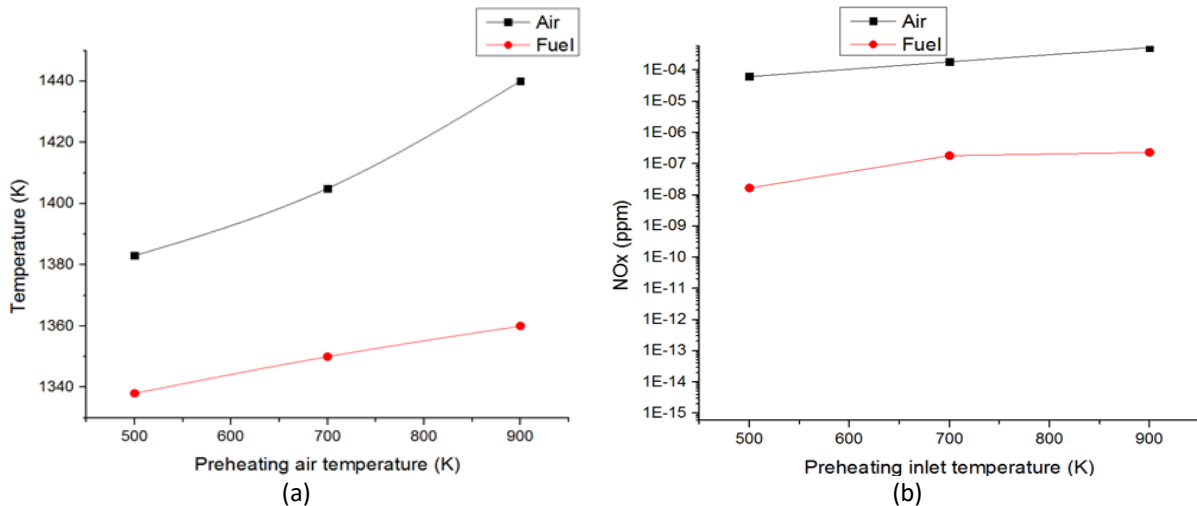


Fig. 15. Effect of preheating fuel and air (a) on temperature combustion, (b) on NOx emission combustion

3.4 Effect of Diluted Air by Using (CO₂ and N₂) Gas on Combustion Temperature and NO_x Emissions at Various Temperatures

Numerous elements can negatively influence the production of NO_x emissions. Diluent gas is one of the techniques, which NO_x emissions can be reduced by using gases (CO₂ and N₂). Diluent gas is a main component of the gas internal flow recirculation (EGR) approach for reducing NO_x emissions through the decreased oxygen concentration. It is used to preheat reactants, which raises the temperature within the combustion chamber above the fuel's auto-ignition temperature to enable flameless combustion.

Figure 16 and Figure 17 show the temperature distribution and the formation of NO_x emissions when using diluted air temperature of CO₂ and N₂ gases at four different air temperatures (T = 300, 500, 700, 900 K) respectively at equivalence ratio ($\Phi=1$). The results of dilution using N₂ and CO₂ gases show that the dilute air preheated using N₂ gas increases the temperature of combustion more than dilute air preheated using CO₂ gas. For diluted CO₂ gas, the minimum temperature of combustion is around 1310K and the minimum temperature of combustion using diluted N₂ gas is 1340 K at the same temperature (T = 300 K) as shown in Figure 16. Results show that minimum NO_x emissions are 9.10×10^{-07} ppm for diluted CO₂ gas. In contrast, minimum NO_x emission at the same temperature (T= 300) on using diluted N₂ gas is 4.2×10^{-06} ppm. In contrast, the maximum temperature of combustion is around 1455K using diluted N₂ gas and the maximum temperature of combustion using diluted CO₂ gas is 1389 K at the same temperature (T =900 K) as shown in Figure 16. Maximum NO_x emissions at temperature (T = 900 K) using N₂ and CO₂ gases are about 4.95×10^{-06} ppm and 6.47×10^{-04} ppm respectively as shown in Figure 17. The CO₂ gas is more effective in reducing NO_x emissions as compared to N₂ gas at various temperatures according to the previous results [8,52-56,64]. By diluting a large amount of flue gas in the reaction zone reduces the effective molecular oxygen concentration, which slows down the kinetic energy and reduces the combustion temperature as heat release decreases [65,66].

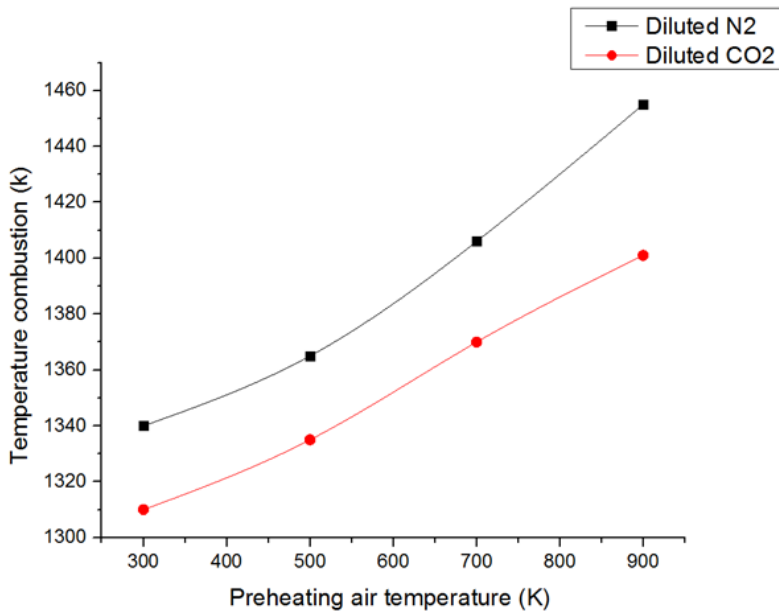


Fig. 16. Effect of preheated air diluted (CO_2 and N_2) on temperature combustion

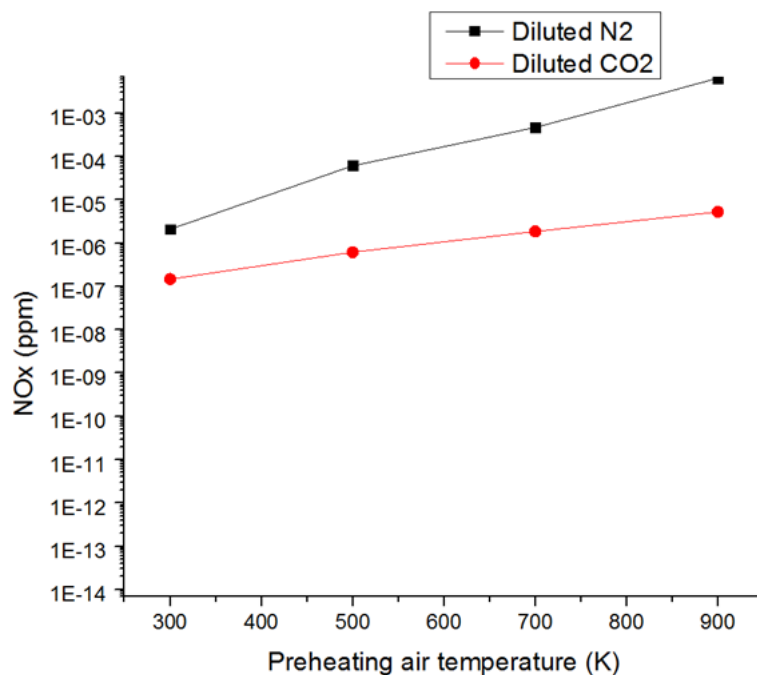


Fig. 17. Effect of preheated air diluted CO_2 and N_2 on NOx (ppm)

Figure 18 and Figure 19 show the effect of preheated dilute of CO_2 and N_2 on temperature distribution on the central axis. Two cases (case one: N_2 is used as a diluent, case two: CO_2 is used as a diluent) have been resolved at the same O_2 concentration (7%). For both cases, the temperature distribution is uniform and decreases towards the combustor outlet due to the gas recirculation. It increases the fuel-air mixture and reduces the high-temperature zone in operation. The temperature distribution is in the range of 1150-1180 K for diluted air using N_2 as compared to 1080-1130 K for diluted air using CO_2 . Moreover, in both cases, as predicted from a distributed reaction in flameless combustion, the thermal field is quite uniform according to a previous study [52,67].

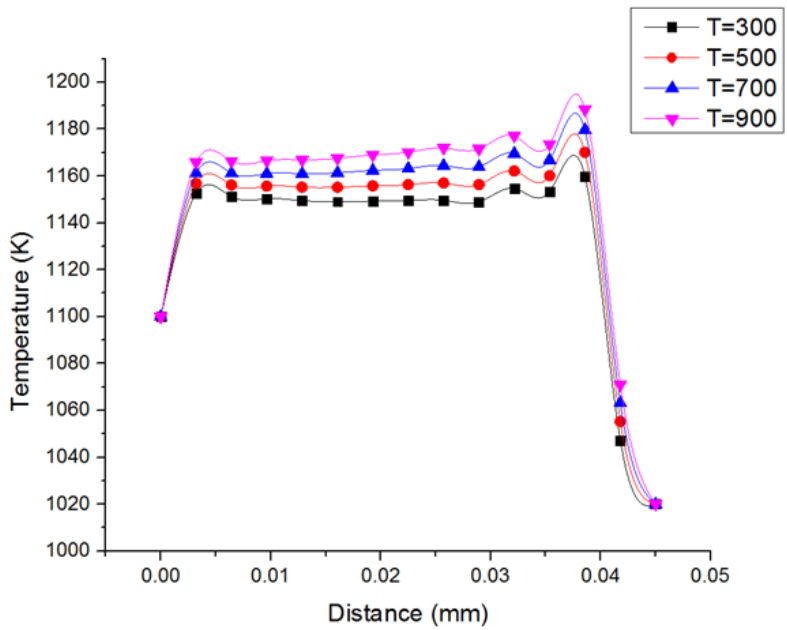


Fig. 18. Effect of preheated diluting air (N₂) on the profile of the central temperature

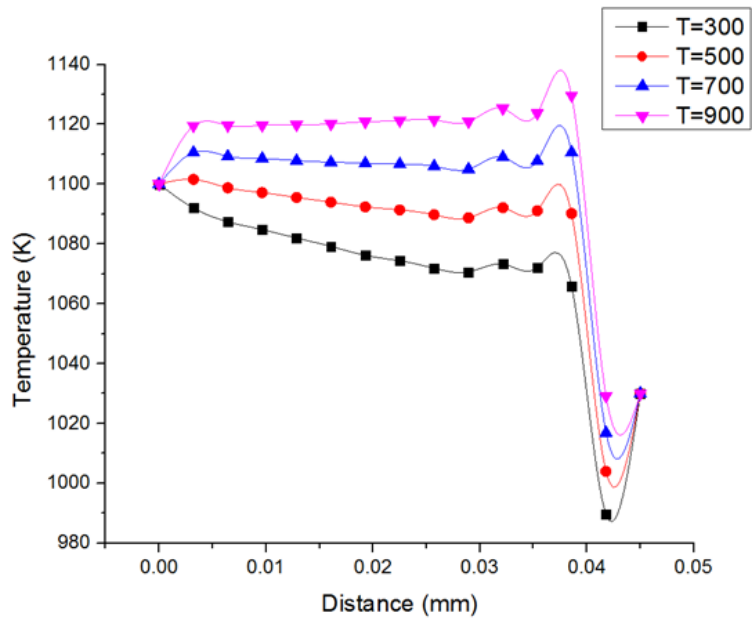


Fig. 19. Effect of preheated diluting air (CO₂) on the profile of the central temperature

Figure 20 and Figure 21 illustrate the distribution and formation of NO_x emissions along the central axis in both cases of dilution with CO₂ and N₂. The NO_x level in Case CO₂ is lower than that in Case N₂ because of the larger reaction zone [52,54]. In general, the distribution of NO_x emissions decreases as the combustion temperature decreases. Whereas, by increasing the temperature of preheated diluted oxidizer results in more NO_x emissions according to previous studies [9].

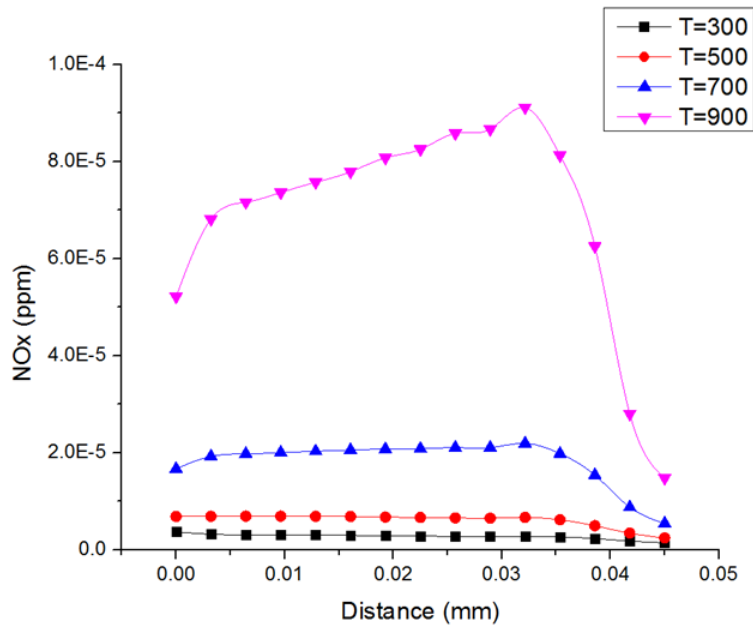


Fig. 20. Effect of preheated diluting air (CO_2) on the central NOx profile

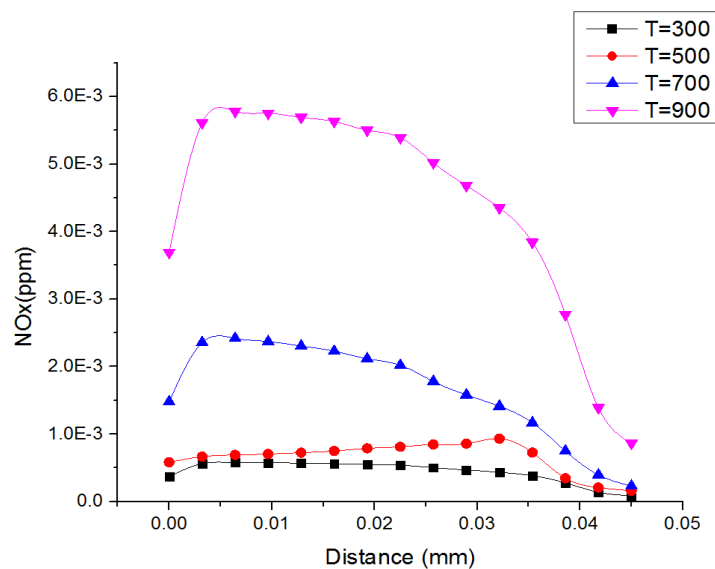


Fig. 21. Effect of preheated diluting air (N_2) on the central NOx profile

The behaviour as seen in the curves is similar but at different value of NOx emission formation. Due to the larger specific heat of CO_2 , turbulence dissipation is increased, peak temperatures are reduced and emissions of thermal NOx are reduced more than used diluted N_2 according to the results of previous studies [52,54]. In general, CO_2 , H_2O , and N_2 diluents are well known in combustion and CO_2 use has been proved to be more effective than N_2 in this research.

3.5 Impact of Tangential Air Location Inlet on Flameless Combustion with Swirling

The flow of air composition plays an important role in controlling and reducing NOx emissions. In this study, forward airflow configurations at different inlet air tangential states and fuel inlet for NOx emissions in flameless vortex combustion were investigated at different flows.

Table 6 shows swirling cases in various configurations. However, the combustor's centreline temperature profile for three different air inlets cases and two fuels inlet using methane gas as a fuel is shown in Figure 22. Many ports are considered important to achieve a good mix of air and fuel. The position of each air and fuel inlet is made for adequate mixing of fuel and air near a strong forced vortex field [30]. In all cases, the temperature distribution is uniform and decreases in all cases towards the combustor outlet due to recirculation. It increases the fuel-air mixture and reduces the high-temperature zone in operation.

Table 6

Various operations of asymmetric vortex based on the position of air and inlet fuel

State	Φ	Number of ports		Location of air		NOx ppm
Without preheated		Fuel	Air	Tangential	Inlet Air	
					Axial	
A3F2	1	2	3	2	1	0.5×10^{-06}
A5F2	1	2	5	4	1	1.8×10^{-06}
A7F2	1	2	7	6	1	4.5×10^{-06}

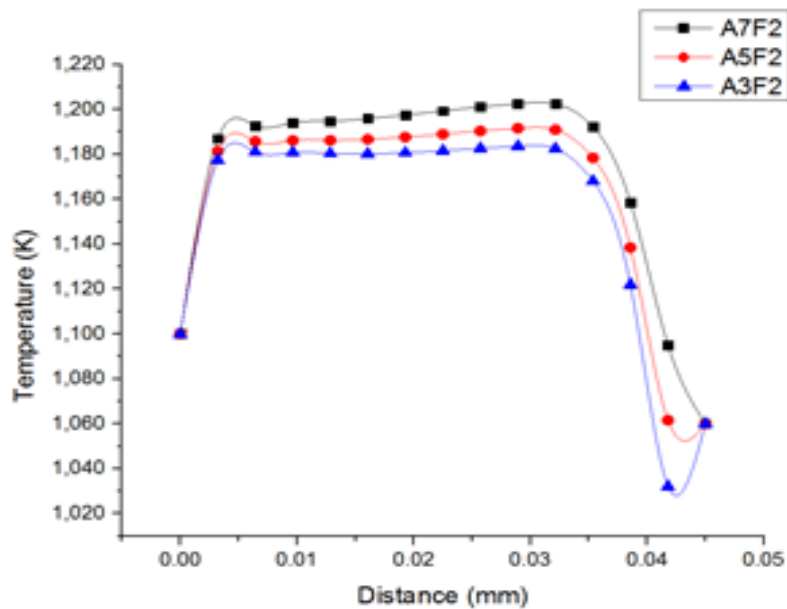


Fig. 22. Temperature spread across the central axis of the chamber at various air inlet tangential states of the combustor with asymmetric

Figure 23 shows the NOx concentration along the central axis in all cases. The NOx level in Case 1 is lower than Case 2 and Case 3. This is because of the lower mass flow rate of air, oxygen concentration, and the increase of velocity in Case 1 [57]. Figure 24 shows the case of 7 air inlet ports. The NOx emissions are higher than in the case of 5 and 3 air inlet ports due to the rise in the obtained airflow rate as a result of an increase in the mixing time between air and fuel according to the previous studies [68]. The study examined multi-injection locations for air and fuel. In that regard, NOx concentrations were greater when multi-port air inlets were relatively used than the other air inlets with fewer ports, according to the previous studies [57,58].

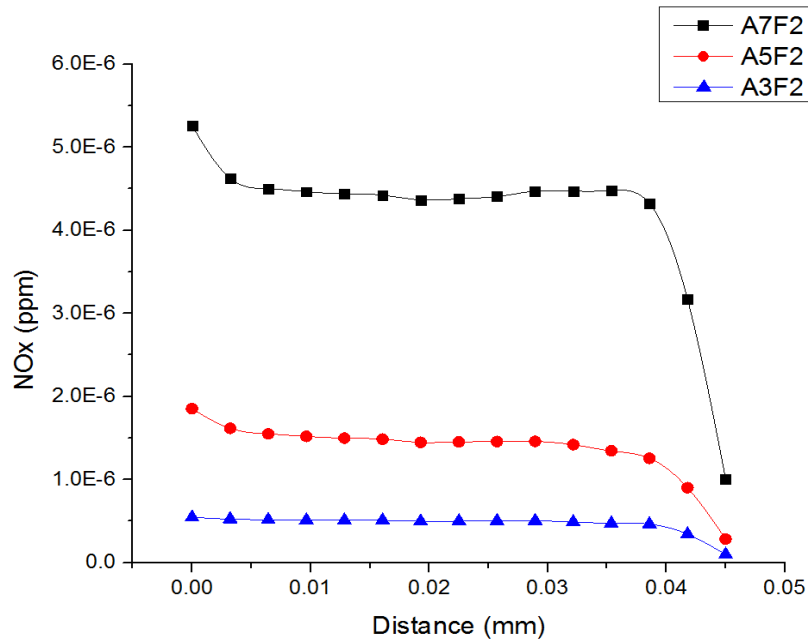


Fig. 23. NOx emission spread across the central axis of the chamber at various air inlet Tangential states of the combustor asymmetric vortex

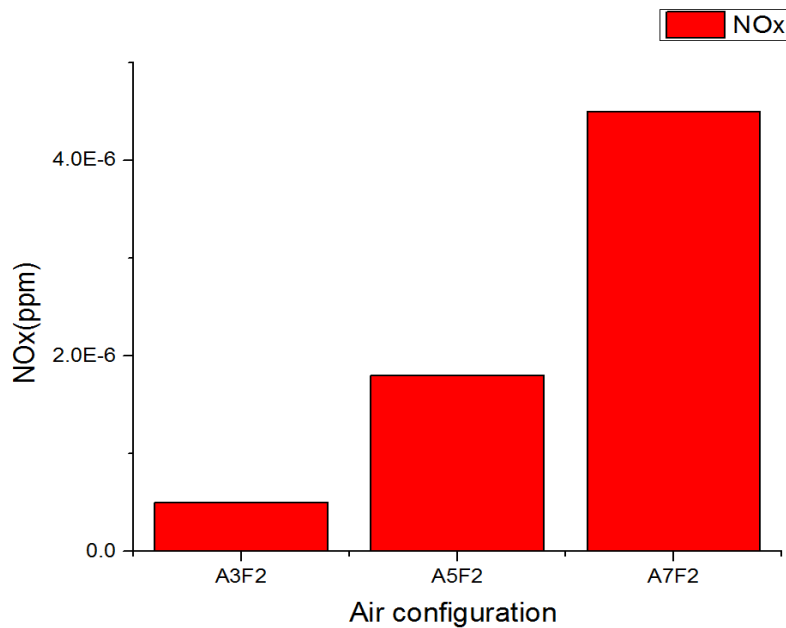


Fig. 24. Average NOx emission under stoichiometric equivalence ratio for asymmetric vortex combustor at various air configurations

The first study on vortex flames was made by Gabler in 1998 [28]. The NOx emission plane in vortex combustion successfully achieved a lower value of emissions as compared to conventional combustion [69]. In this article, the investigation aims to obtain the emission characteristics of methane fuel under a swirl flameless combustor by using CO₂ and N₂ gases as the diluent at different temperatures to find better results of reducing NOx emission. In addition, it investigates the effect of preheating air and fuel on NOx emission. They are important and effective parameters of the robust design method, which successfully reduce the NOx emissions and achieve flameless.

4. Conclusion

An analysis study using simulation on the efficiency of asymmetric vortex flameless for several entrances tangential air location at various oxygen concentrations together with the impact on preheating air and fuel was performed. The investigation on the effect of preheated diluted air on NO_x emission was also considered. The obtained results were divided into three groups according to the number of air inlet ports (7 ports) and two fuel inlets. Many ports were considered important to achieve a good mixture of air and fuel. The results showed that by increasing the inlet tangential air had a significant effect on the increase of combustion temperature and NO_x emission. More so, NO_x emissions were higher with an application of 7-port air inlets as compared to 5 and 3. The results showed that by increasing oxygen concentration leads to an increase in temperature of combustion and NO_x emissions. Also, it was observed that the oxygen concentration had a minimal effect on NO_x when the equivalent ratios Φ were 1 and 1.2 as compared to the oxygen concentration of 0.5. The same result can be achieved by increasing the preheated air temperature. However, better results in reducing NO_x emissions were recorded from preheated air dilution with CO₂ when compared to preheated air dilution with N₂. In general, preheated air and fuel are technologies that play an important role in establishing.

References

- [1] Rosec, Žiga, Tomaž Katrašnik, Urban Žvar Baškovič, and Tine Seljak. "Exhaust gas recirculation with highly oxygenated fuels in gas turbines." *Fuel* 278 (2020): 118285. <https://doi.org/10.1016/j.fuel.2020.118285>
- [2] Liu, Wen, Ziqu Ouyang, Xiaoyang Cao, and Yongjie Na. "The influence of air-stage method on flameless combustion of coal gasification fly ash with coal self-preheating technology." *Fuel* 235 (2019): 1368-1376. <https://doi.org/10.1016/j.fuel.2018.08.127>
- [3] Wang, G., J. Si, M. Xu, and J. Mi. "MILD combustion versus conventional bluff-body flame of a premixed CH₄/air jet in hot coflow." *Energy* 187 (2019): 115934. <https://doi.org/10.1016/j.energy.2019.115934>
- [4] Wüning, J. A., and J. G. Wüning. "Flameless oxidation to reduce thermal NO-formation." *Progress in Energy and Combustion Science* 23, no. 1 (1997): 81-94. [https://doi.org/10.1016/S0360-1285\(97\)00006-3](https://doi.org/10.1016/S0360-1285(97)00006-3)
- [5] Gupta, Ashwani K. "Thermal characteristics of gaseous fuel flames using high temperature air." *Journal of Engineering for Gas Turbines and Power* 126, no. 1 (2004): 9-19. <https://doi.org/10.1115/1.1610009>
- [6] Arghode, Vaibhav K., and Ashwani K. Gupta. "Role of thermal intensity on operational characteristics of ultra-low emission colorless distributed combustion." *Applied Energy* 111 (2013): 930-956. <https://doi.org/10.1016/j.apenergy.2013.06.039>
- [7] Augusto Viviani Perpignan, A. A. V., A. Gangoli Rao, and D. J. E. M. Roekaerts. "Flameless combustion and its potential towards gas turbines." *Progress in Energy and Combustion Science: An International Review Journal* 69 (2018). <https://doi.org/10.1016/j.pecs.2018.06.002>
- [8] Tu, Yaojie, Wenming Yang, Keng Boon Siah, and Subbaiah Prabakaran. "A comparative study of methane MILD combustion in O₂/N₂, O₂/CO₂ and O₂/H₂O." *Energy Procedia* 158 (2019): 1473-1478. <https://doi.org/10.1016/j.egypro.2019.01.352>
- [9] Mehregan, Mina, and Mohammad Moghiman. "A numerical investigation of preheated diluted oxidizer influence on NO_x emission of biogas flameless combustion using Taguchi approach." *Fuel* 227 (2018): 1-5. <https://doi.org/10.1016/j.fuel.2018.04.049>
- [10] Khidr, Kareem I., Yehia A. Eldrainy, and Mohamed M. EL-Kassaby. "Towards lower gas turbine emissions: Flameless distributed combustion." *Renewable and Sustainable Energy Reviews* 67 (2017): 1237-1266. <https://doi.org/10.1016/j.rser.2016.09.032>
- [11] Fordoei, E. Ebrahimi, and Kiumars Mazaheri. "Effects of preheating temperature and dilution level of oxidizer, fuel composition and strain rate on NO emission characteristics in the syngas moderate or intense low oxygen dilution (MILD) combustion." *Fuel* 285 (2021): 119118. <https://doi.org/10.1016/j.fuel.2020.119118>
- [12] Zhu, Shu-Jun, Qing-Gang Lyu, Jian-Guo Zhu, and Jia-Rong Li. "NO emissions under pulverized char MILD combustion in O₂/CO₂ preheated by a circulating fluidized bed: Effect of oxygen-staging gas distribution." *Fuel Processing Technology* 182 (2018): 104-112. <https://doi.org/10.1016/j.fuproc.2018.09.002>
- [13] Gurunathan, Balamurugan A., Uswah Khairuddin, Nazrun Nabill Azlan Shah, and Ricardo Martinez-Botas. "Influence of Double Entry Volute on Incidence Angle Variation Under Steady Flow: Numerical Investigation." *CFD Letters* 12,

- no. 10 (2020): 75-89. <https://doi.org/10.37934/cfdl.12.10.7589>
- [14] Zikri, Ahmad, Engkos Achmad Kosasih, Muhammad Irfan Dzaky, and Firdaus Firdaus. "Combination of Dehumidifier, Heat Pump and Air Heater: Influence of Temperature, Specific Humidity, And Mass Flow Rate of Air on Specific Energy Consumption." *Journal of Advanced Research in Fluid Mechanics and Thermal Sciences* 76, no. 1 (2020): 124-134. <https://doi.org/10.37934/arfmts.76.1.124134>
- [15] Hosseini, Seyed Ehsan, Hasan Barzegaravval, Bruce Chehroudi, and Mazlan Abdul Wahid. "Hybrid solar flameless combustion system: Modeling and thermodynamic analysis." *Energy Conversion and Management* 166 (2018): 146-155. <https://doi.org/10.1016/j.enconman.2018.04.012>
- [16] Zhu, Shanglong, Artur Pozarlik, Dirk Roekaerts, Hugo Correia Rodrigues, and Theo van der Meer. "Numerical investigation towards HiTAC conditions in laboratory-scale ethanol spray combustion." *Fuel* 211 (2018): 375-389. <https://doi.org/10.1016/j.fuel.2017.09.002>
- [17] Sorrentino, Giancarlo, Pino Sabia, Mara de Joannon, Pio Bozza, and Raffaele Ragucci. "Influence of preheating and thermal power on cyclonic burner characteristics under mild combustion." *Fuel* 233 (2018): 207-214. <https://doi.org/10.1016/j.fuel.2018.06.049>
- [18] Fan, Aiwu, He Zhang, and Jianlong Wan. "Numerical investigation on flame blow-off limit of a novel microscale Swiss-roll combustor with a bluff-body." *Energy* 123 (2017): 252-259. <https://doi.org/10.1016/j.energy.2017.02.003>
- [19] Li, PengFei, JianChun Mi, B. B. Dally, FeiFei Wang, Lin Wang, ZhaoHui Liu, Sheng Chen, and ChuGuang Zheng. "Progress and recent trend in MILD combustion." *Science China Technological Sciences* 54, no. 2 (2011): 255-269. <https://doi.org/10.1007/s11431-010-4257-0>
- [20] Weber, Roman, Ashwani K. Gupta, and Susumu Mochida. "High temperature air combustion (HiTAC): How it all started for applications in industrial furnaces and future prospects." *Applied Energy* 278 (2020): 115551. <https://doi.org/10.1016/j.apenergy.2020.115551>
- [21] Stănilă, Marius-Ion, and Valentin Nedeff. "Trends regarding the development of high thermic efficiency and low level of polluting emissions combustion systems." *Journal of Engineering Studies and Research* 19, no. 1 (2013): 61-67. <https://doi.org/10.29081/jesr.v19i1.141>
- [22] Hosseini, Seyed Ehsan, and Mazlan Abdul Wahid. "Investigation of bluff-body micro-flameless combustion." *Energy Conversion and Management* 88 (2014): 120-128. <https://doi.org/10.1016/j.enconman.2014.08.023>
- [23] Hosseini, Seyed Ehsan, and Mazlan Abdul Wahid. "Enhancement of exergy efficiency in combustion systems using flameless mode." *Energy Conversion and Management* 86 (2014): 1154-1163. <https://doi.org/10.1016/j.enconman.2014.06.065>
- [24] Alwan, Raid A., M. Wahid, A. Abuelnuor, and Mohd Suardi. "Combustion in asymmetric vortex chambers." In *International Conference on Energy and Thermal Sciences*. 2014.
- [25] Khaleghi, Mostafa, S. E. Hosseini, M. A. Wahid, and H. A. Mohammed. "The Effects of Air Preheating and Fuel/Air Inlet Diameter on the Characteristics of Vortex Flame." *Journal of Energy* 2015 (2015). <https://doi.org/10.1155/2015/397219>
- [26] Kumar, P. K. Ezhil, and D. P. Mishra. "Numerical investigation of the flow and flame structure in an axisymmetric trapped vortex combustor." *Fuel* 102 (2012): 78-84. <https://doi.org/10.1016/j.fuel.2012.06.056>
- [27] Kasani, Adam, Mazlan Abdul Wahid, Ahmad Dairobi Ghazali, and Mohammed Bashir Abdulrahman. "The Effects of Multiple Swirl Generator Inlets Circumferential Distribution to a Liquid Fuelled Ultra-High Swirl Flameless Combustion Characteristics." *Journal of Advanced Research in Fluid Mechanics and Thermal Sciences* 76, no. 2 (2020): 65-74. <https://doi.org/10.37934/arfmts.76.2.6574>
- [28] Gabler, Hampton Clay. "An experimental and numerical investigation of asymmetrically-fueled whirl flames." *PhD diss., Princeton University*, 1998.
- [29] Ishak, Mohamad Shaiful Ashrul, and Mohammad Nazri Mohd Jaafar. "Numerical Analysis on the CO-NO Formation Production near Burner Throat in Swirling Flow Combustion System." *Jurnal Teknologi* 69, no. 2 (2014): 71-77. <https://doi.org/10.11113/jt.v69.3110>
- [30] Al Wan, Raid Abid. "Thermal and Fluid Flow Analysis of Swirling Flameless Combustion." *PhD diss., Universiti Teknologi Malaysia*, 2016.
- [31] Alwan, Raid Abid, Mazlan Abdul Wahid, Mohd Fairus Mohd Yasin, Arkan Al-Taie, and Abuelnuor Abdeen Ali Abuelnuor. "Effects of equivalence ratio on asymmetric vortex combustion in a low nox burner." *International Review of Mechanical Engineering (IREME)* 9, no. 5 (2015): 476-483. <https://doi.org/10.15866/ireme.v9i5.7157>
- [32] Alwan, Raid A., M. Wahid, A. Abuelnuor, and Arkan Al Taie. "NOx Characteristics in Asymmetric Vortex Combustion." In *7th International Meeting on Advanced Thermofluids (IMAT 2014)*, Kuala Lumpur-Malaysia. 2014.
- [33] Saqr, Khalid M., Hossam S. Aly, Mohsin M. Sies, and Mazlan A. Wahid. "Computational and experimental investigations of turbulent asymmetric vortex flames." *International Communications in Heat and Mass Transfer* 38, no. 3 (2011): 353-362. <https://doi.org/10.1016/j.icheatmasstransfer.2010.12.001>

- [34] ANSYS. "ANSYS Fluent Theory Guide Release 16.0, SAS IP." *ANSYS Inc* 894 (2015): 895.
- [35] Saqr, Khalid M., Hossam S. Aly, Mazlan A. Wahid, and Mohsin M. Sies. "Numerical Simulation of Confined Vortex Flow Using a Modified $k-\epsilon$ Turbulence Model." *CFD Letters* 1, no. 2 (2009): 87-94.
- [36] Saqr, Khalid M., Hossam S. Aly, Hassan I. Kassem, Mohsin M. Sies, and Mazlan A. Wahid. "Computations of shear driven vortex flow in a cylindrical cavity using a modified $k-\epsilon$ turbulence model." *International Communications in Heat and Mass Transfer* 37, no. 8 (2010): 1072-1077. <https://doi.org/10.1016/j.icheatmasstransfer.2010.06.021>
- [37] Sies, Mohsin Mohd, and Mazlan Abdul Wahid. "Numerical investigation of the asymmetrical vortex combustor running on biogas." *Journal of Advanced Research in Fluid Mechanics and Thermal Sciences* 74, no. 1 (2020): 1-18. <https://doi.org/10.37934/arfmts.74.1.118>
- [38] Turns, Stephen R. *Introduction to combustion*. Third ed. New York, NY, USA: McGraw-Hill Companies, 1996.
- [39] Westbrook, Charles K., and Frederick L. Dryer. "Simplified reaction mechanisms for the oxidation of hydrocarbon fuels in flames." *Combustion Science and Technology* 27, no. 1-2 (1981): 31-43. <https://doi.org/10.1080/00102208108946970>
- [40] Bagheri, Ghobad, Ehsan Hamidi, Mazlan A. Wahid, Aminuddin Saat, and Mohsin M. Sies. "Effects of CO₂ Dilution on the Premixed Combustion of CH₄ in Microcombustor." In *Applied Mechanics and Materials*, vol. 388, pp. 251-256. Trans Tech Publications Ltd, 2013. <https://doi.org/10.4028/www.scientific.net/AMM.388.251>
- [41] Hosseini, Seyed Ehsan, Ghobad Bagheri, and Mazlan Abdul Wahid. "Numerical investigation of biogas flameless combustion." *Energy Conversion and Management* 81 (2014): 41-50. <https://doi.org/10.1016/j.enconman.2014.02.006>
- [42] Danon, B., E-S. Cho, W. De Jong, and D. J. E. M. Roekaerts. "Numerical investigation of burner positioning effects in a multi-burner flameless combustion furnace." *Applied Thermal Engineering* 31, no. 17-18 (2011): 3885-3896. <https://doi.org/10.1016/j.applthermaleng.2011.07.036>
- [43] Xing, Fei, Arvind Kumar, Yue Huang, Shining Chan, Can Ruan, Sai Gu, and Xiaolei Fan. "Flameless combustion with liquid fuel: A review focusing on fundamentals and gas turbine application." *Applied Energy* 193 (2017): 28-51. <https://doi.org/10.1016/j.apenergy.2017.02.010>
- [44] Wu, Ming-hsun, Yanxing Wang, Vigor Yang, and Richard A. Yetter. "Combustion in meso-scale vortex chambers." *Proceedings of the Combustion Institute* 31, no. 2 (2007): 3235-3242. <https://doi.org/10.1016/j.proci.2006.08.114>
- [45] Khaleghi, Mostafa, Seyed Ehsan Hosseini, and Mazlan Abdul Wahid. "Emission and combustion characteristics of hydrogen in vortex flame." *Jurnal Teknologi* 66, no. 2 (2014): 47-51. <https://doi.org/10.11113/jt.v66.2483>
- [46] Saqr, Khalid M., Hossam S. Aly, Mohsin M. Sies, and Mazlan A. Wahid. "Effect of free stream turbulence on NO_x and soot formation in turbulent diffusion CH₄-air flames." *International Communications in Heat and Mass Transfer* 37, no. 6 (2010): 611-617. <https://doi.org/10.1016/j.icheatmasstransfer.2010.02.008>
- [47] Gupta, Ashwani, and Toshiaki Hasegawa. "The effect of air preheat temperature and oxygen concentration in air on the structure of propane air diffusion flames." In *37th Aerospace Sciences Meeting and Exhibit*, p. 725. 1999. <https://doi.org/10.2514/6.1999-725>
- [48] Hosseini, Seyed Ehsan, and Mazlan Abdul Wahid. "Biogas utilization: Experimental investigation on biogas flameless combustion in lab-scale furnace." *Energy Conversion and Management* 74 (2013): 426-432. <https://doi.org/10.1016/j.enconman.2013.06.026>
- [49] Hosseini, Seyed Ehsan. "Experimental and Numerical Analyses of Flameless Combustion Using Biogas from Palm Oil Mill Effluent." *PhD diss., Universiti Teknologi Malaysia*, 2016.
- [50] Gupta, A. K., S. Bolz, and T. Hasegawa. "Effect of air preheat temperature and oxygen concentration on flame structure and emission." *Journal of Energy Resources Technology* 121, no. 3 (1999): 209-216. <https://doi.org/10.1115/1.2795984>
- [51] Abuelnuor, A. A. A., M. A. Wahid, H. A. Mohammed, and A. Saat. "Flameless combustion role in the mitigation of NO_x emission: a review." *International Journal of Energy Research* 38, no. 7 (2014): 827-846. <https://doi.org/10.1002/er.3167>
- [52] Cho, Eun-Seong, and Suk-Ho Chung. "Experiment on Low NO_x Combustion Characteristics by Flue Gas Dilution In Air and Fuel Sides." In *Proceedings of the KSME Conference*, pp. 1499-1504. The Korean Society of Mechanical Engineers, 2004.
- [53] Abuelnuor, Abuelnuor Abdeen Ali. "Thermal characteristics and emissions of gaseous fuel flameless combustion with tangential air inlet." *PhD diss., Universiti Teknologi Malaysia*, 2014.
- [54] Feser, Joseph S., Serhat Karyeyen, and Ashwani K. Gupta. "Flowfield impact on distributed combustion in a swirl assisted burner." *Fuel* 263 (2020): 116643. <https://doi.org/10.1016/j.fuel.2019.116643>
- [55] Yuan, Jianwei, and Ichiro Naruse. "Effects of air dilution on highly preheated air combustion in a regenerative furnace." *Energy & Fuels* 13, no. 1 (1999): 99-104. <https://doi.org/10.1021/ef980127y>
- [56] Lille, Simon, Włodzimierz Blasiak, and Marcin Jewartowski. "Experimental study of the fuel jet combustion in high temperature and low oxygen content exhaust gases." *Energy* 30, no. 2-4 (2005): 373-384.

- <https://doi.org/10.1016/j.energy.2004.05.008>
- [57] Alwan, Raid A., M. A. Wahid, Mohd Fairus M. F., A. A. Abuelnuor, and Arkan Al Taie. "The effect of swirling vortex combustion on NOX emissions." *Recent Advances in Mechanics and Mechanical Engineering* (2015): 62-66.
- [58] Wang, C. T., and Y. C. Hu. "Mixing of liquids using obstacles in y-type microchannels." *Journal of Applied Science and Engineering* 13, no. 4 (2010): 385-394.
- [59] Katsuki, Masashi, and Toshiaki Hasegawa. "The science and technology of combustion in highly preheated air." In *Symposium (International) on Combustion*, vol. 27, no. 2, pp. 3135-3146. Elsevier, 1998. [https://doi.org/10.1016/S0082-0784\(98\)80176-8](https://doi.org/10.1016/S0082-0784(98)80176-8)
- [60] Li, Hejie, Ahmed Elkady, and Andrei Evulet. "Effect of exhaust gas recirculation on NOx formation in premixed combustion system." In *47th AIAA Aerospace Sciences Meeting Including The New Horizons Forum and Aerospace Exposition*, p. 226. 2009. <https://doi.org/10.2514/6.2009-226>
- [61] Choi, Gyung-Min, and Masashi Katsuki. "Advanced low NOx combustion using highly preheated air." *Energy Conversion and Management* 42, no. 5 (2001): 639-652. [https://doi.org/10.1016/S0196-8904\(00\)00074-1](https://doi.org/10.1016/S0196-8904(00)00074-1)
- [62] Verissimo, A. S., A. M. A. Rocha, P. J. Coelho, and M. Costa. "Experimental and numerical investigation of the influence of the air preheating temperature on the performance of a small-scale mild combustor." *Combustion Science and Technology* 187, no. 11 (2015): 1724-1741. <https://doi.org/10.1080/00102202.2015.1059330>
- [63] Liu, Changchun, Shien Hui, Su Pan, Denghui Wang, Tong Shang, and Ling Liang. "The influence of air distribution on gas-fired coal preheating method for NO emissions reduction." *Fuel* 139 (2015): 206-212. <https://doi.org/10.1016/j.fuel.2014.08.068>
- [64] Lyu, Qing-Gang, Shu-Jun Zhu, Jian-Guo Zhu, Hui-Xing Wu, and Yan-Qi Fan. "Experimental study on NO emissions from pulverized char under MILD combustion in an O₂/CO₂ atmosphere preheated by a circulating fluidized bed." *Fuel Processing Technology* 176 (2018): 43-49. <https://doi.org/10.1016/j.fuproc.2018.03.008>
- [65] Gupta, Ashwani K. "Thermal characteristics of gaseous fuel flames using high temperature air." *Journal of Engineering for Gas Turbines and Power* 126, no. 1 (2004): 9-19. <https://doi.org/10.1115/1.1610009>
- [66] Abuelnuor, A. A. A., M. A. Wahid, Seyed Ehsan Hosseini, A. Saat, Khalid M. Saqr, Hani H. Sait, and M. Osman. "Characteristics of biomass in flameless combustion: A review." *Renewable and Sustainable Energy Reviews* 33 (2014): 363-370. <https://doi.org/10.1016/j.rser.2014.01.079>
- [67] Li, Pengfei, Bassam B. Dally, Jianchun Mi, and Feifei Wang. "MILD oxy-combustion of gaseous fuels in a laboratory-scale furnace." *Combustion and Flame* 160, no. 5 (2013): 933-946. <https://doi.org/10.1016/j.combustflame.2013.01.024>
- [68] Khalil, Ahmed EE, Vaibhav K. Arghode, and Ashwani K. Gupta. "Novel mixing for ultra-high thermal intensity distributed combustion." *Applied Energy* 105 (2013): 327-334. <https://doi.org/10.1016/j.apenergy.2012.12.071>
- [69] Yu, Byeonghun, Sung-Min Kum, Chang-Eon Lee, and Seungro Lee. "Study on the combustion characteristics of a premixed combustion system with exhaust gas recirculation." *Energy* 61 (2013): 345-353. <https://doi.org/10.1016/j.energy.2013.08.057>